IRis

Northeastern University

Electrical and Computer Engineering Faculty Publications

Department of Electrical and Computer Engineering

April 01, 1994

Measurements of surface impedance, London penetration depth, and coherence length in YBaCuO films at microwave-frequencies

H. Jiang

T. Yuan

H. How

A. Widom
Northeastern University

C. Vittoria
Northeastern University

See next page for additional authors

Recommended Citation

Jiang, H.; Yuan, T.; How, H.; Widom, A.; Vittoria, C.; Chrisey, D.; Horwitz, J.; and Drehman, A., "Measurements of surface impedance, London penetration depth, and coherence length in YBaCuO films at microwave-frequencies" (1994). *Electrical and Computer Engineering Faculty Publications.* Paper 83. http://hdl.handle.net/2047/d20002254

This work is available open access, hosted by Northeastern University.

Author(s)
H. Jiang, T. Yuan, H. How, A. Widom, C. Vittoria, D. Chrisey, J. Horwitz, and A. Drehman

This article is available at IRis: http://iris.lib.neu.edu/elec_comp_fac_pubs/83

Measurements of surface impedance, London penetration depth, and coherence length in Y-Ba-Cu-O films at microwave frequencies

H. Jiang, T. Yuan, H. How, A. Widom, and C. Vittoria
Northeastern University, Boston, Massachusetts 02115

D. Chrisey and J. Horwitz
Naval Research Laboratory, Washington, D.C. 20375

A. Drehman
Rome Laboratory, Hanscom Air Force Base, Massachusetts 01731
(Received 8 June 1992; revised manuscript received 12 November 1993)

We have improved a microwave self-resonant technique to measure surface resistance R_s directly and surface inductance L_s indirectly. For films prepared by the laser ablation technique we observed that R_s at 21 GHz decreased by about three orders of magnitude as the temperature decreased from 90 to 80 K reaching a low value of 4.9×10^{-4} Ω. We measured the London penetration depth λ and coherence length ξ, and found that both λ and ξ are anisotropic. Their values depended on the direction of the microwave electric field relative to the *c* axis. We deduced the value of $\lambda_{\parallel}(0)$ to be about 1800 Å, $\lambda_{\parallel}(86.5)$ about 8000 Å, and $\lambda_{\perp}(86.5)$ about 26 000 Å, where $\lambda_{\parallel}(0)$ is the penetration depth (as $T\rightarrow0$ K) for the electromagnetic electric field parallel and $\lambda_{\perp}$ perpendicular to the film plane. In addition $\xi_{\parallel}$ was determined to be 129 Å and $\xi_{\perp}$ equal to 40 Å at 86.5 K. The anisotropic factor γ is about 3.

I. INTRODUCTION

Since the discovery of superconductivity in high-T_c materials,[1] the measured value of the surface resistance R_s of Y-Ba-Cu-O at microwave frequencies has decreased steadily.[2–7] The reduction in R_s is a reflection on the improved quality of films and measurement capabilities. The implication from recent measurements[2,5–7] is that the intrinsic limits of R_s and related parameters are within the limit of measurability with present techniques. As such, we believe that it is timely now to infer fundamental properties of the superconducting state of Y-Ba-Cu-O from measurements of R_s and related parameters.

In this paper we improve upon a microwave self-resonant (MSR) technique to measure R_s directly and L_s, the surface inductance, indirectly. From R_s and L_s we deduce the London penetration depth λ, and the coherence length ξ. Also, electron paramagnetic resonance (EPR) techniques are used to deduce λ and ξ. We compare the MSR technique with conventional coplanar waveguide (CPW) resonator and waveguide cavity techniques in the measurements of R_s. The microwave measurements were correlated with dc field measurements using a vibrating sample magnetometer (VSM) apparatus. These sets of measurements provided a consistent set of measurements which formed the basis of our study: the measurement of the fundamental length scales of Y-Ba-Cu-O in the superconducting state.

We determined that both λ and ξ are anisotropic. Their values depended on the direction of the microwave electric field relative to the *c* axis. We determined the anisotropy factor to be about 3. This result was in good agreement with other published results.[8–10,31,32] The significant information reported here is the quantitative measure of both λ and ξ. It appears that the value of $\lambda_{\parallel}(0)$ is about 1800 Å, where $\lambda_{\parallel}$ is defined as the penetration depth parallel to the film plane or perpendicular to the *c* axis. $\lambda_{\perp}(86.5)$ is measured by us to be equal to 26 000 Å.

We also report $\xi_{\parallel}$ and $\xi_{\perp}$, where $\xi_{\parallel}$ is defined as the coherence length applicable for the electric field (or current) applied along the *a*-*b* plane and $\xi_{\perp}$ is along the *c* axis. At $T=86.5$ K, $\xi_{\parallel}=129$ Å and $\xi_{\perp}=40$ Å. The microwave techniques used here are not able to deduce ξ below 77 K, since the *B* field internal to the film was approximately constant below this temperature. The coherence length usually is deduced from the measurement of upper critical magnetic field H_{c2}.[8–10] However, H_{c2} of Y-Ba-Cu-O is extremely high; the measurement requires special and difficult techniques.

In Sec. II, we discuss the sample preparation and characterization. In Sec. III we discuss our measurement technique to measure R_s and L_s. Comparison of our techniques with others is given in Sec. IV. The experimental results are discussed in Sec. V, followed by discussions and conclusions.

II. SAMPLE PREPARATION AND CHARACTERIZATION

Pulsed laser ablation was used to deposit films of $YBa_2Cu_3O_{7-\delta}$. The deposition technique may be briefly described. The output of a Lambda Physik model 315 excimer laser operating at 248 nm (KrF) was focused with a 50-cm-focal-length lens to an energy density of 1.5 J/cm^2

 ©1994 The American Physical Society

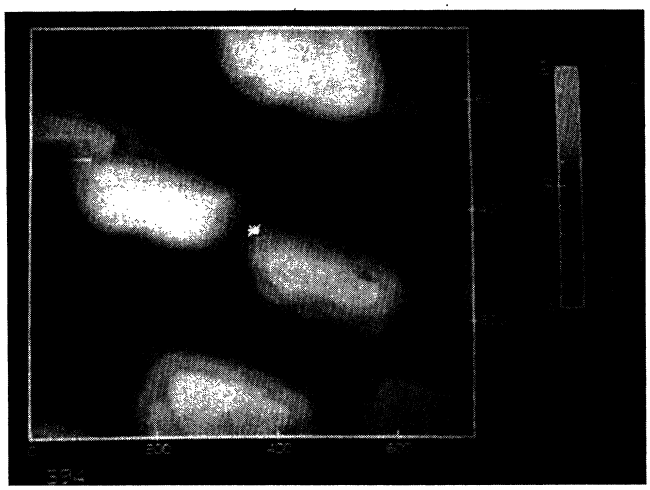

FIG. 1. STM micrograph of a superconducting film. The vertical and horizontal axes are in units of mm; each division is 200 nm.

onto a stoichiometric $YBa_2Cu_3O_{7-\delta}$ target. The targets were commercially purchased and were specified to be 99.999% pure. The ablated material was deposited onto a heated (100)-oriented MgO substrate positioned ~4 cm from the target. The substrate was held at 750 °C in 300 mTorr of oxygen atmosphere during the deposition and then quenched to room temperature in 1 atm of oxygen. The deposition rate was ~1 Å/pulse over a 1-cm^2 substrate area. The film thickness was measured using a Dektak mechanical transducer, and typically we obtained ~5000-Å-thick films. The room-temperature resistivity of the films was about 300 $\mu\Omega$ cm. The transition temperature was measured using the four-probe method, and typical T_c was about 90 K; the transition width was about 0.5 K. These results were fairly reproducible from run to run. In our characterization studies, as many as 10–156 sample films were used for our investigation. We defined T_c as the temperature at which the resistance was half of the onset value. The dc transport measurements were made inductively using a multiturn coil pressed against the film to induce surface currents. Changes in the coil's inductance and the third harmonic of the driving voltage were used to determine J_c.[11] The current densities exceeded 10^6 A/cm^2 at 77 K. X-ray diffraction indicated that the films were oriented with the c axis normal to the substrate surface. The reader is referred to Ref. 12 for actual display of x-ray data of our film. Pole figure analysis of (012) peaks, for similar films, indicated a continuum of a-b in-plane misorientations peaked strongly at 90° and a much lesser extent at 45°. Scanning tunneling microscope (STM) analysis indicates a surface roughness of the order of < 500 Å (see Fig. 1).

III. MICROWAVE EXPERIMENTAL TECHNIQUES

A. Microwave self-resonant technique

This technique was initially reported by Skrehot and Chang[13] to measure the ratio of surface resistance of a superconductor and characteristic impedance of a waveguide at resonant frequency. In Ref. 13 an analysis was developed only at the resonant frequency. We have extended the analysis to be applicable at resonance as well as off resonance. As a result, R_s, L_s, C, and Z_0 were determined uniquely from our analysis, where R_s is the surface resistance of the superconducting strip, L_s is the surface inductance due to the superconducting screening currents, C is the capacitance due to the gap between the strip and the waveguide, and Z_0 is the characteristic impedance of the waveguide. From these parameters the penetration depth and coherence length of the superconducting films were deduced. A thin-film strip (4.24×0.9 mm^2) of Y-Ba-Cu-O was placed in a waveguide whose cross section was 10.67×4.32 mm^2 as shown in Fig. 2. The thickness of the film was typically 0.5 μm. The equivalent circuit of the strip and waveguide transmission line is also shown in Fig. 2. A typical gap value was 0.04 mm, and it corresponded to $C\simeq10^{-12}f$. No systematic study was made to relate the gap width with C. However, besides the gap the dielectric constant of the substrate on which the Y-Ba-Cu-O film was deposited affected the value of C. We empirically varied the width of the gap until the transmission microwave resonance was observed between 18 and 26 GHz, the fundamental band of propagation in the waveguide.

The inductance L was a combination of the superconductor intrinsic inductance L_s and the self inductance L_0, calculated approximately as[14]

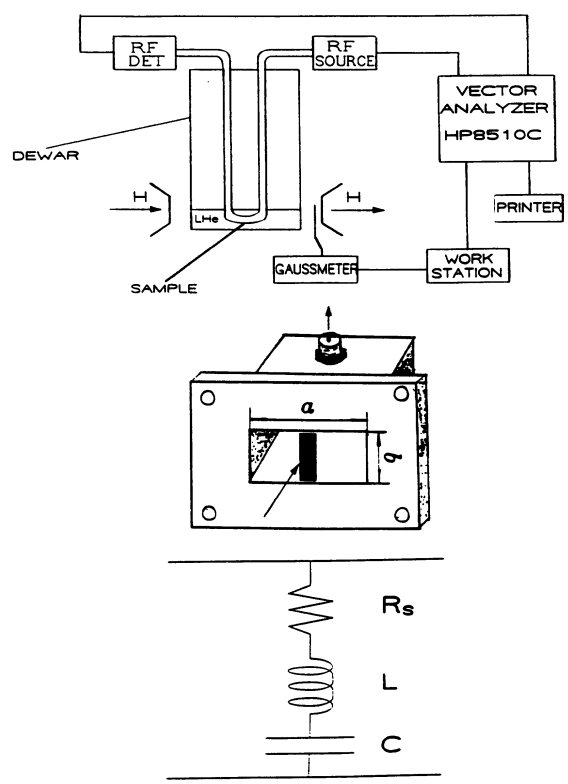

FIG. 2. Schematic of microwave self-resonant experiment and equivalent circuit of the MSR measurement.

$$L_0 \simeq \frac{Z_0}{2\pi f_0}\frac{a}{b}\frac{f}{\sqrt{f_c^2-f^2}}\left[\sin\frac{3\pi}{2}\left[\frac{\sin x}{x}\right]\right]^2\left[1-\frac{w}{a}\right], \tag{1}$$

where

$$x=\frac{3\pi}{2}\frac{w}{a}, \quad f_c=\frac{3c}{2a},$$

and

$$w=0.9 \text{ mm}, \quad a=10.67 \text{ mm}, \quad b=4.32 \text{ mm}.$$

f_0 is the transmission resonant frequency, and c is the speed of light. A typical value of L_0 was $\sim 10^{-11}$ H. In comparison to L_0, L_s was about a factor of 100 lower.

From the equivalent circuit of Fig. 2, the reflection S_{11} and transmission S_{21} coefficients may be calculated as follows:

$$S_{11}=-\left[\frac{2Z}{Z_0}+1\right]^{-1}=|S_{11}|e^{j\phi_{11}} \tag{2}$$

and

$$S_{21}=\left[\frac{Z_0}{2Z}+1\right]^{-1}=|S_{21}|e^{j\phi_{21}}, \tag{3}$$

where ϕ_{11} and ϕ_{21} are the phase angles of S_{11} and S_{21}. For the equivalent circuit of Fig. 2,

$$Z=R_s+i\left[\omega L-\frac{1}{\omega C}\right]; \tag{4}$$

putting (4) into (3), we get

$$S_{21}=\frac{(\omega/\omega_0)R_s\sqrt{C/L}+i[(\omega/\omega_0)^2-1]}{(\omega/\omega_0)(R_s+Z_0/2)\sqrt{C/L}+i[(\omega/\omega_0)^2-1]}, \tag{5}$$

where

$$\omega_0=\frac{1}{\sqrt{LC}} \tag{6}$$

is the transmission resonant frequency. Letting

$$y=\frac{\omega}{\omega_0}, \tag{7}$$

$$\gamma^2=\frac{C}{L}R_s^2, \tag{8}$$

and

$$\eta^2=\frac{C}{L}\left[\frac{Z_0}{2}\right]^2, \tag{9}$$

(5) can be written as

$$S_{21}=\frac{\gamma y+i(y^2-1)}{(\gamma+\eta)y+i(y^2-1)}. \tag{10}$$

The amplitude and phase are, respectively (we used $|S_{21}|^2$ instead of $|S_{21}|$ for simplifying the fitting procedure),

$$P=|S_{21}|^2=\frac{\gamma^2y^2+(y^2-1)^2}{y^2(\gamma+\eta)^2+(y^2-1)^2}, \tag{11}$$

$$\phi_{21}=\tan^{-1}\left[\frac{1-y^2}{\gamma y}\right]-\tan^{-1}\left[\frac{1-y^2}{(\gamma+\eta)y}\right]. \tag{12}$$

By fitting the experimental curves, the parameters γ and η and, therefore R_s and L can be deduced. At resonant frequency, the imaginary part vanishes; hence $Z=R_s$. R_s may be determined from (3) directly,

$$R_s=\frac{Z_0}{2[1/|S_{21}|-1]}. \tag{13}$$

It is noted that in (13) there is no other loss parameter in the expression. Loss tangents of the substrate have minimal effects on the measurement of R_s. For example, we have included realistic loss tangents for a typical substrate material of MgO or $SrTiO_3$, etc., and calculated $|S_{21}|$. The correction to R_s [using (13)] from the loss tangent contribution was calculated to be about 0.04% at 80 K (using MgO as an example).

The surface impedance Z for a finite-thickness strip is determined from

$$Z=-jZ_\infty\cot\left[\frac{\omega\mu_0 d}{Z_\infty}\right]. \tag{14}$$

The subscript ∞ is to denote that as $d\to\infty$, $Z\to Z_\infty$;

$$Z_\infty=R_s+i\left[\omega L-\frac{1}{\omega C}\right]. \tag{15}$$

As in any development of a new technique, we calibrated the measurement with standard materials, such as films of copper, silver, etc. We placed strips of copper, silver, aluminum, and bulk Y-Ba-Cu-O in the waveguide for the purpose of determining Z_0 and to measure the conductivity of each material. Z_0 determined from calibration runs was 43 Ω. Conceivably, L_0 could have been determined from the calibration runs, since L_0 was not a property of the superconducting material. However, this would require identical strip dimensions and substrate material for both Y-Ba-Cu-O and the reference material. Instead, we determined L_0 from f_0 and line-shape fitting of $|S_{21}|$ versus frequency for each run under consideration.

The limitation of this technique was dependent on the sensitivity of the HP8510 network analyzer. For example, by amplifying the transmitted signal with a 20-dB amplifier, the sensitivity of the technique can be improved so that a surface resistance as small as 20 μΩ can be measured.

B. EPR absorption technique

Normally, in an EPR measurement technique, dP/dH is measured,[15] where P is the microwave power absorbed by the sample in question and H is the magnetic field. The EPR technique was used[15] in the past to measure dP/dH at low-H fields on superconducting high-T_c materials. This technique was often referred to in the litera-

ture[16] as the "magnetically modulated microwave absorption," (MMMA) technique. We introduced this technique to measure dP/dH in 1987 (Ref. 16) in order to measure T_c of very fine particle of Y-Ba-Cu-O. In that experiment dP/dH was measured as a function of temperature. Since the introduction of that technique, we have developed an analysis of the line shape of dP/dH as a function of H to deduce $\lambda_\perp/\xi_\perp$ and $\lambda_\perp$. A superconducting sample of Y-Ba-Cu-O was placed inside a microwave cavity and allowed to cool down below T_c. By sweeping the external magnetic field between ± 200 Oe, dP/dH was measured as a function of H.

For a single fluxoid core region in a type-II superconductor, P_1 is given as

$$P_1 = \sigma_n E_0^2 \pi \xi^2 t \ , \tag{16}$$

where σ_n is the normal conductivity and E_0 is the external microwave electric field along the fluxoid axis (which is normal to the film). ξ is the coherence length, and t is the film thickness. For a long cylinder, such as a fluxoid in which the diameter to length ratio is small, the external and internal electric fields are equal, since the depolarization factor is zero. If there are more fluxoids and one can assume a square lattice of fluxoids, then the total power absorbed is simply

$$P = NP_1 = \frac{A}{D^2} P_1 \ , \tag{17}$$

where A is the total area of the film and D is the flux lattice constant. As it is well known,[17] D is related to B, the magnetic flux density, by the relationship

$$\frac{1}{D^2} = \frac{|B|}{\phi_0} \ . \tag{18}$$

Thus Eq. (17) becomes

$$P = (A \sigma_0 E_0^2 \pi t / \phi_0) \xi^2 |B| \equiv C_1 \xi^2 |B| \ . \tag{19}$$

In the superconducting region, the microwave electric field, relative to E_0, is reduced by a factor of $\sigma_s/\omega\epsilon_0$, which is of the order of 10^5. For this case the depolarization factor is 1, since the aspect ratio is much greater than 1. However, one could still have attenuating fields adjacent to the fluxoid region. This implies that both the electromagnetic **e**, electric, and **h**, magnetic, fields extend beyond the fluxoid core. When we allow for attenuating fields, we obtain, for P,

$$P = C_1 |B| \left[1 - \left[\frac{\delta_1 D}{\xi^2} + \frac{\delta_1^2}{2\xi^2} \right] \exp(-2D/\delta_1) + \left[\frac{\delta_1}{\xi} + \frac{\delta_1^2}{2\xi^2} \right] \exp(-2\xi/\delta_1) \right] \ , \tag{20}$$

where $\delta_1 = \mathrm{Re}(\delta)$, with

$$\frac{1}{\delta^2} = \frac{1}{\delta_0^2} + \frac{1}{\lambda^2} \ . \tag{21}$$

λ is the penetration depth of the superconductor. δ_0 is the normal skin depth and is equal to

$$\frac{1}{\delta_0^2} = -\frac{4\pi i \omega \sigma_n}{c^2} \ . \tag{22}$$

In the MMMA experiment, one measures dP/dH or

$$\frac{dP}{dH} = \frac{dP}{dB} \frac{dB}{dH} \ . \tag{23}$$

dP/dB was calculated from Eq. (20), but dB/dH was obtained from VSM measurement of M versus H or

$$\frac{dB}{dH} = 1 + 4\pi\alpha \frac{dM}{dH} \ , \tag{24}$$

where $\alpha \approx 0.009$ is the measured demagnetization factor. The c axis for all of our films was aligned perpendicular to the film plane. By combining these two microwave techniques, we were able to measure the penetration depth along the two directions relative to the c axis.

C. Coplanar waveguide technique

In this technique we measured the reflection coefficient S_{11}. The amplitude of S_{11} is given as[18]

$$|S_{11}| = \left[\frac{(K-1)^2 + 4Q_0(f/f_0 - 1)^2}{(K+1)^2 + 4Q_0(f/f_0 - 1)^2} \right]^{1/2} \ , \tag{25}$$

where f_0 is the resonant frequency of the resonator, K is the coupling coefficient, and Q_0 = unloaded Q. The change in the inverse of Q_0 is related to the total resistance R_T,

$$\Delta \left[\frac{1}{Q_0} \right] \propto R_s + R_\epsilon + R_r + R_w = R_T \ , \tag{26}$$

where R_s is the surface resistance of the superconductor, R_ϵ is related to the loss tangent of the substrate, R_r is related to the radiation resistance, and R_w is related to the surface wave losses.

Usually, in order to measure R_s reliably and accurately with this technique, one needs to minimize $R_\epsilon + R_r + R_w$. Since our main emphasis here was to measure λ, the penetration depth, we have developed a simple analysis in which λ is deduced without determining R_s:

$$\lambda = G \frac{\Delta f}{f_0} \ , \tag{27}$$

where G is a constant evaluated in Ref. 18 and Δf is the change in resonant frequency of the resonator at two temperatures relatively close to f_0. Thus we had three techniques at our disposal which were used to generate a set of consistent data.

IV. COMPARISON WITH OTHER TECHNIQUES

Clearly, R_s may be measured by other microwave techniques. Our main interest was to establish intrinsic values of R_s at any temperature and frequency however determined by experimental techniques. As such, we compared our techniques with others in order to obtain a reasonable value of R_s. In this section we are addressing the following question: Given that one can adequately

TABLE I. Comparison of sensitivities.

Technique	Lowest R_s ($\mu\Omega$)	Frequency (GHz)	Reference
Cavity	400	10	2
CPW stripline	~1000	10	18,19
Parallel plate	5	10	3
Split-ring resonator	<10	1.78	5
Dielectric resonator	50	18.7	7
MSR	20	21	

measure the appropriate microwave quantity, what is the lowest value of R_s that one can deduce from a given technique?

For techniques similar to the CPW technique, such as stripline and microstrip, the reader is referred to Refs. 19–21. Surface resistances determined from these techniques are dependent on the quality factor Q and frequency, $R_s \sim f/Q$.[19,20] At 10 GHz, these techniques can only measure surface resistance of the order of ~ 1 mΩ.[19,20]

A technique often deployed by others is the so-called "cavity" technique, and the reader is referred to Refs. 22–24. Basically, the loaded Q and change in resonance frequency, Δf, are measured. The loaded Q may be related to the unloaded Q by determining the coupling K in a similar manner as in the previous section. In the cavity technique, $R_r = R_w = 0$, so that

$$\Delta\left[\frac{1}{Q_0}\right] \propto R_s + R_c + R_h \ , \tag{28}$$

where R_c is the surface resistance of the cavity walls and R_h is the contribution from the sample holder. Presently, superconducting cavities are used so that $(R_c + R_h) \sim R_s$. From f_0 it may be possible to deduce $L_s + L_c$, where L_s is the inductance of the superconducting specimen and L_c the inductance of the cavity walls and self-inductance. Usually, $L_c \gg L_s$ by as much as 10^3. To our knowledge values of L_s have not been reported by this technique. The limitation of the surface resistance of the cavity technique is from the background Q; the best surface resistance measurable by this technique is about 400 $\mu\Omega$ at 10 GHz.[2]

The reader is referred to Ref. 3 for details of the parallel-plate resonator technique. For this technique again the unloaded Q and resonant frequency are measured. Here $R_c = R_h = 0$, but one needs to contend with the dielectric loss tangent. Specifically, Taber[3] found that

$$\frac{1}{Q_0} = \tan\delta + \beta R_s/S + \alpha S \ , \tag{29}$$

where S is the spacing between the parallel plates, α and β are coefficients depending on the geometry of the resonator, and $\tan\delta = \epsilon''/\epsilon'(\epsilon = \epsilon' - j\epsilon'')$. As stated by Taber, S and $\tan\delta$ could be purposely chosen to make the second term in Eq. (29) the dominant term. Thus the lower limit of R_s depends on the selection of substrate material. The lowest surface resistance that can be measured by this technique is about 5 $\mu\Omega$ at 10 GHZ. Again, it may be possible to use Eq. (29) to deduce L_s.

Other techniques, such as the split-ring resonator[5] and dielectric resonator,[7] have the same type of analysis as above. The lowest values of surface resistances are of the order of <10 and 50 $\mu\Omega$, respectively.

Finally, we summarize the lower limits of surface resistance R_s that can be measured by various techniques in Table I. As can be seen in Table I, intrinsic values of R_s can indeed fall below the threshold of measurability for the "cavity" method and stripline technique but not for the MSR and other techniques.

V. EXPERIMENTAL RESULTS

In Fig. 3 we plot measured $20\log_{10}|S_{21}|$ and ϕ_{21} as a function of normalized frequency and the temperature is near T_c. The data are represented by points and the least-squares fit by a solid line. The following parameters were deduced from the fit at $T = 86$ K: $L = 2.8\times10^{-11}h$, $C = 2.05\times10^{-12}f$, and $R_s = 0.052$ Ω. Since our interest was to deduce R_s and L_s from the raw data, we adopted the following procedure: R_s was obtained at resonance using Eq. (13). The value of L_s was deduced from

$$L_s(T+\Delta T) - L_s(T) = -2\frac{\Delta f}{f_0}L \ , \tag{30}$$

where we assumed that the frequency shift was only due to the superconducting strip. Frequency shifts were mea-

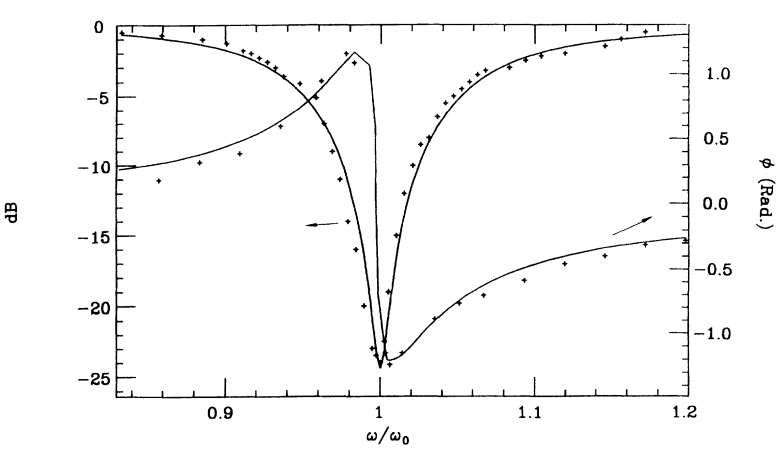

FIG. 3. Amplitude in dB and phase angle of transmission coefficient as a function of normalized frequency at 86 K for a Y-Ba-Cu-O strip. The resonant frequency is 21 GHz. The solid line is a fitting curve.

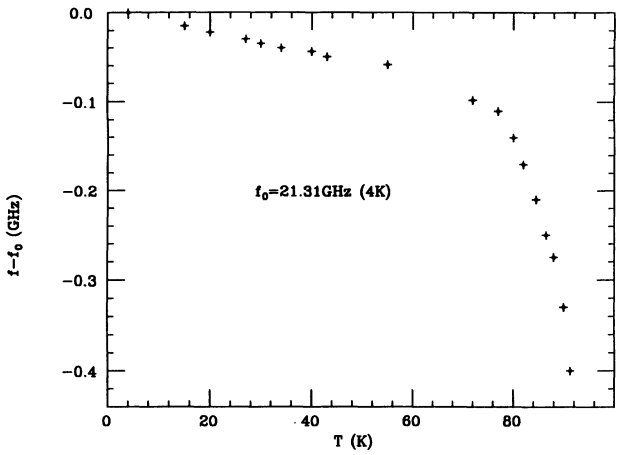

FIG. 4. Frequency shift of a Y-Ba-Cu-O strip with respect to the resonant frequency at 4 K.

sured with respect to the resonant frequency at 4 K (see Fig. 4). L_s at 4 K can also be deduced from the surface resistance R_s. Since $R_s=\frac{1}{2}\mu_0^2\sigma_n\omega^2\lambda^3$ and $X_s=\omega L_s=\omega\mu_0\lambda$,

$$L_s=\left[\frac{2\mu_0 R_s}{\omega^2\sigma_n}\right]^{1/3} . \tag{31}$$

This served as a reference point for the rest of the data of L_s at higher temperatures.

In Fig. 5, R_s and L_s are plotted as a function of temperature, R_s decreased by about three orders of magnitude as the temperature decreased from 90 to 80 K, reaching a low value of 4.9×10^{-4} Ω. At 15 K, R_s was 2.7×10^{-4} Ω, the lowest value measured using the MSR method. If we extrapolate[5] R_s to lower frequencies, we find that R_s is equivalent to 100 μΩ at 10 GHz and 8.7 μΩ at 2.95 GHz. The temperature is assumed to be equal to 77 K. However, at 15 K, the extrapolated values would be 61 μΩ at 10 GHz and 5.3 μΩ at 2.95 GHz. A comparison with other measurements of R_s is given in Tables II and III. We note that our measured values of R_s exhibit an oscillating behavior with temperature, although L_s does not. We do not attribute the oscillatory behavior of R_s to an intrinsic process, since lower values of R_s have been measured at lower frequencies (10 GHz) (Refs. 3 and 4) and no oscillatory behavior of R_s was observed.

Assuming that the surface impedance is of the form

$$Z_s=R_s+j\omega L_s=j\omega\mu_0\left[\lambda^2-j\left[\frac{\rho_n}{\mu_0\omega}\right]\right]^{1/2} , \tag{32}$$

we can solve for λ and ρ_n and obtain the relations:

$$\lambda=\frac{1}{\mu_0\omega}\sqrt{X_s^2-R_s^2} \tag{33}$$

and

$$\rho_n=\frac{2}{\mu_0\omega}X_sR_s . \tag{34}$$

In Fig. 6 we plot λ as a function of temperature. Typical values of λ are 1800 Å at 4 K and 8000 Å at 86.5 K, for example. We have fitted λ to a Gorter-Casimir two-fluid model,[25]

$$\lambda(T)=\lambda(0)\left[1-\left[\frac{T}{T_c}\right]^4\right]^{-1/2} . \tag{35}$$

The results are shown in Fig. 6 with a dashed line. If we change the power factor in Eq. (35) from 4 to 2, we obtain a better fitting curve (see solid line in Fig. 6).

We also measured the penetration depth λ(0) from the shift in the resonant frequency with temperature using a CPW resonator; it was again 1800 Å. We have not included plots of R_T by the CPW technique, since most of its contribution is due to radiation resistance or surface wave losses.

The penetration depth near T_c was also measured by EPR or by the so-called MMMA technique.[26] The basic assumption of the analysis is that the microwave absorp-

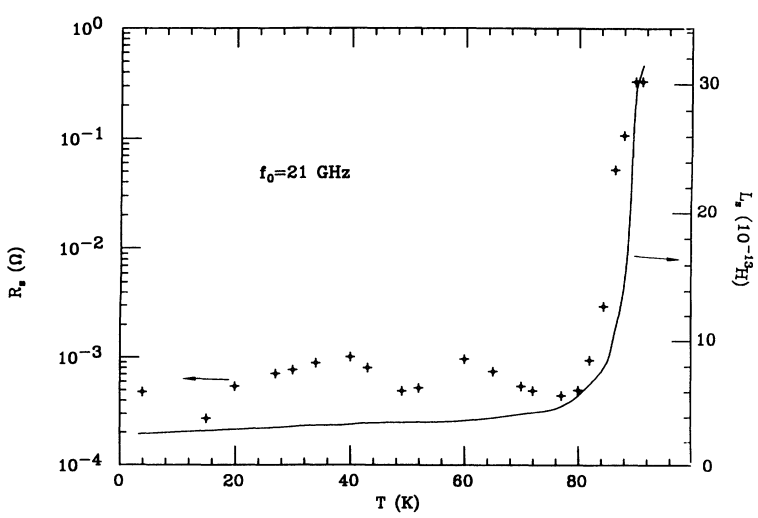

FIG. 5. Surface resistance and inductance of a Y-Ba-Cu-O strip as a function of temperature.

TABLE II. Summary of results at $T=77$ K.

Technique	R_s ($\mu\Omega$)	L_s ($10^{-13}h$)	λ (Å)	f (GHz)	Sample	Reference
	441	4.79	3817	21		our
A	100[a]			10	film	MSR
	8.7[a]			2.95		technique
B	1500			18.7	film	7
C	720			10	film	3
D	22			2.95	crystal	5

[a]We have scaled R_s as $\propto f^2$.

TABLE III. Summary of results at $T=4$ K.

Technique	R_s ($\mu\Omega$)	L_s (10^{-13})h	λ (Å)	f (GHz)	Sample	Reference
	480[a]	2.33	1800	21		our
A	108[b]			10	film	MSR
	9[b]			2.95		technique
B	60			18.7	film	7
C	56		1400	10	film	3
D	15 (1.7 K)			2.95	crystal	5
D	<400		1600	10	crystal	2
F	12–180		1400	10	film	6
G	20–43			10	film	4

[a]We measured $R_s=270\ \mu\Omega$ at 15 K and at 21 GHz.
[b]We have scaled R_s as $\propto f^2$.

TABLE IV. Summary of λ, ξ, and κ. The accuracy of our measurements is within $\pm5\%$.

T (K)	$\lambda_\parallel$ (Å)	$\xi_\parallel$ (Å)	$\kappa_\perp$	$\lambda_\perp$ (Å)	$\xi_\perp$ (Å)	$\lambda_\perp/\xi_\perp$	$\kappa_\parallel$	Reference
86.5	8000[a]	129[a]	62	26 000[b]	40[b]	650[b]	200	our measurements
0	1800[a]	25[c]	72		8[b,c]			our measurements
0	950	22	44	7800	6.7	1164	230	8
0	260	34	7.6	1250	7	178	37	9
0		16.4	52–60		3		350–410	10
0		31 (crystal)			4.3 (crystal)			30
		13 (film)			2 (film)			
0	1415			>7000				31
0	1400	20	70					32,33
0	1400	22	64					34
0	1500							35

[a]MSR result.
[b]EPR result.
[c]Extrapolated from 86.5 K.

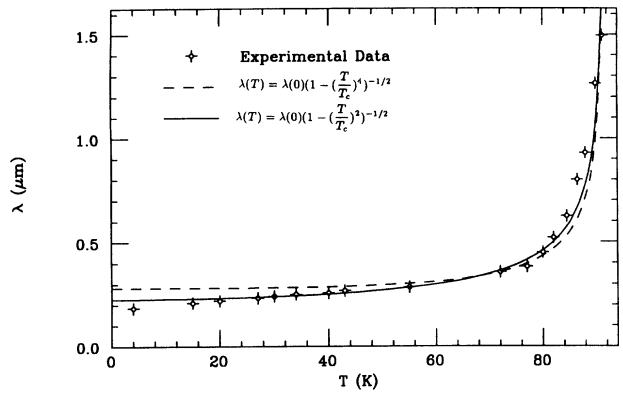

FIG. 6. London penetration depth $\lambda_{\parallel}$ deduced from MSR measurements as a function of temperature. The dashed line is a fitting curve using the two-fluid model, and the solid line is $\lambda(T)=\lambda(0)[1-(T/T_c)^2]^{-1/2}$.

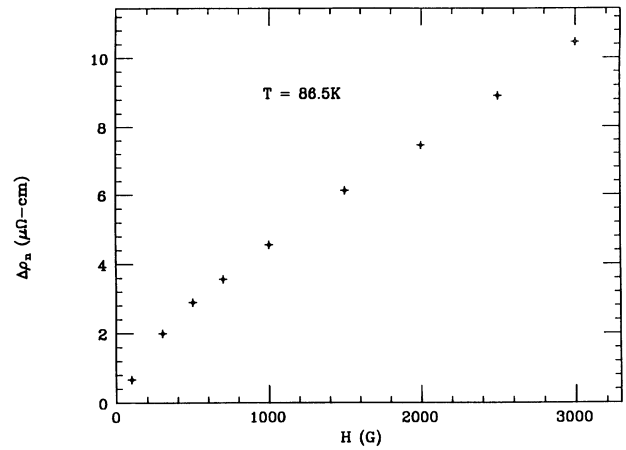

FIG. 8. Changes of resistivity as a function of magnetic fields.

tion scales as the B field or the volume of the normal region. Shown in Fig. 7 are measured and calculated dP/dH as a function of H. In this fit, we deduced $\lambda=26\,000$ Å and $\xi=40$ Å at 86.5 K. However, a clear distinction is to be pointed out here. Data for λ generated in MSR and CPW resonator measurements assume the microwave electric field to be parallel to the film plane. We denote them as $\lambda_{\parallel}$. For the MMMA case, the data are denoted as $\lambda_{\perp}$, since the microwave electric field is parallel to the c axis. The same definitions for $\xi_{\parallel}$ and $\xi_{\perp}$ apply. The anisotropy in λ and ξ was most conveniently described by an anistorpic Ginzburg-Landau parameter κ, and it was defined as[27,28]

$$\kappa_{\perp}=\lambda_{\parallel}/\xi_{\parallel} , \tag{36}$$

$$\kappa_{\parallel}=(\lambda_{\parallel}\lambda_{\perp})^{1/2}/(\xi_{\parallel}\xi_{\perp})^{1/2} . \tag{37}$$

The anisotropy of these parameters are determined by the anisotropy factor γ,

$$\kappa_{\parallel}=\gamma\kappa_{\perp} , \tag{38}$$

$$\xi_{\parallel}=\gamma\xi_{\perp} , \tag{39}$$

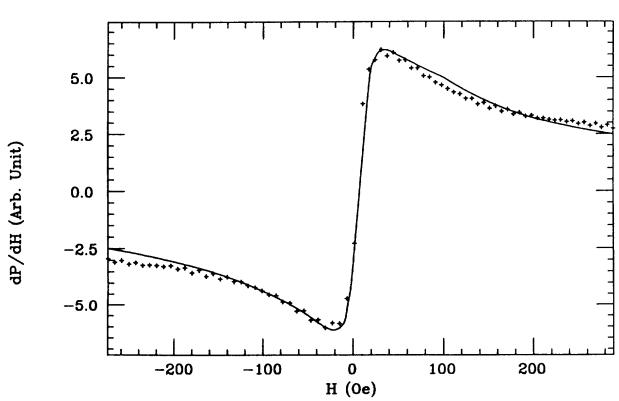

FIG. 7. dP/dH as a function of H by using the MMMA technique. The points are experimental data, and the curve is calculated from the fluxoid model.

and

$$\lambda_{\parallel}=\lambda_{\perp}/\gamma . \tag{40}$$

The coherence length and penetration depth are also defined as[29] $\xi=(\xi_a\xi_b\xi_c)^{1/3}$ and $\lambda=(\lambda_a\lambda_b\lambda_c)^{1/3}$, and since $\xi_a\simeq\xi_b$ and $\lambda_a\simeq\lambda_b$ for Y-Ba-Cu-O, we can write $\xi=(\xi_{\parallel}^2\xi_{\perp})^{1/3}$ and $\lambda=(\lambda_{\parallel}^2\lambda_{\perp})^{1/3}$.

In deducing $\xi_{\parallel}$ from the MSR technique, we needed to apply a magnetic field H parallel to the c axis or perpendicular to the film plane. We found that R_s changed with H, but L_s remained constant for fields up to 3 kOe. Changes of resistivity calculated from surface resistance changes due to magnetic fields are shown in Fig. 8. Using the Bardeen-Stephens relationship

$$(\xi)^2=\frac{\Delta\rho_n\phi_0\sigma_n}{\pi B} , \tag{41}$$

and Eq. (34), we determined $\xi_{\parallel}=129$ Å at 86.5 K with corresponding value of $\kappa_{\perp}\simeq 62$, where we treat B as approximately equal to $\mu_0 H$. Below 77 K, we were not able to measure significant changes in R_s with respect to the application of a magnetic field. Hence no estimate of $\xi_{\parallel}$ was obtained. If we extrapolate our results to $T\rightarrow 0$ K by using the relation $\xi=\xi(0)(1-T/T_c)^{-1/2}$, we find that $\xi_{\parallel}(0)$ to be 25 Å with a corresponding value of $\kappa_{\perp}\simeq 72$. In Table IV we report our deduced values of $\xi_{\parallel}$, $\xi_{\perp}$, $\lambda_{\parallel}$, $\lambda_{\perp}$, $\kappa_{\parallel}$, and $\kappa_{\perp}$ from our MSR and EPR measurements and from measurements and calculations by others.[8–10,29–35]

VI. DISCUSSION AND CONCLUSIONS

We have used three different microwave techniques to measure R_s, L_s, λ, ξ, and κ. The measurements overall are consistent with each other and reveal that λ, ξ, and κ are anisotropic. Our measurements give an anisotropy factor γ of roughly ~ 3, which is in general agreement with other reports. The values of λ and ξ depend on the direction of the electric field or supercurrent relative to the c axis. This in itself is not new, since recent results[8–10] have indicated as much. However, in this paper

we have tried to obtain consistent quantitative results. Specifically, we have determined that for the current density **J**, the direction perpendicular to the c axis, $\xi_{\parallel}$, is 129 Å at 86.5 K and extrapolates to 25 Å at 0 K if we use the relationship $\xi(T)=\xi(0)(1-T/T_c)^{-1/2}$. For **J** along the c axis, $\xi_{\perp}$ is 40 Å at 86.5 K and extrapolates to 8 Å at 0 K.

A summary of the measured characterizing parameters of a Y-Ba-Cu-O film are given in Table IV in comparison with others' results. Umezawa *et al.*[8] and Worthington, Gallagher, and Dinger[9] measured the penetration depth and coherence length in both the c and a-b directions. From their results, one concluded an anisotropic factor γ of 3–5; however, their measured penetration depths λ's at 0 K were smaller than the λ's measured by others[31–35] and us. Harshman *et al.*[31] measured the penetration depth along both directions, but no coherence length data were obtained. $\lambda_{\parallel}$ and $\xi_{\parallel}$ reported in Refs. 32–34 were consistent; they measured $\lambda_{\parallel}=1400$ Å and $\xi_{\parallel}=20\sim22$ Å. However, no data along the c-axis direction were available for comparison.

We do not believe that the above values of ξ's we obtained represent their intrinsic limit. This is because we measured $\lambda_{\parallel}\simeq1800$ Å at 4 K; however, many groups[31–33] have reported $\lambda_{\parallel}(0)$ to be about 1400 Å. If we assume the latter value of $\lambda_{\parallel}$ to be intrinsic, we extrapolate the following values for $\xi_{\parallel}$ and $\xi_{\perp}$, respectively, at 0 K: 19 and 6 Å.

ACKNOWLEDGMENTS

We would thank Professor J. Krim for taking the STM picture. We also thank the NSF for supporting this work.

[1]K. W. Blazey, K. A. Muller, J. G. Bednorz, and W. Berlinger, Phys. Rev. B **36**, 7241 (1987).
[2]D. Wu, W. Kennedy, C. Zahopoulos, and S. Sridhar, Appl. Phys. Lett. **55**, 698 (1989).
[3]R. C. Taber, Rev. Sci. Instrum. **61**, 2200 (1990).
[4]P. Merchant, R. Jacowitz, K. Tibbs, R. Taber, and S. Laderman, Appl. Phys. Lett. **60**, 763 (1992).
[5]D. A. Bonn, P. Dosanjh, R. Liang, and W. N. Hardy, Phys. Rev. Lett. **68**, 2390 (1992).
[6]D. Miller, L. Richards, S. Etemad, A. Inam, T. Vankatesan, B. Dutta, X. Wu, C. Eom, T. Geballe, N. Newman, and B. Cole, Appl. Phys. Lett. **59**, 2326 (1991).
[7]N. Klein, U. Dahne, U. Poppe, N. Tellmann, K. Urban, S. Orbach, S. Hensen, G. Muller, and H. Piel, J. Superconduct. **5**, 195 (1992).
[8]A. Umezawa, G. Crabtree, J. Liu, T. Moran, S. Malik, L. Nunez, W. Kwok, and C. Swoers, Phys. Rev. B **38**, 2834 (1988).
[9]T. Worthington, W. Gallagher, and T. Dinger, Phys. Rev. Lett. **59**, 1160 (1987).
[10]U. Welp, W. Kwok, G. Crabtree, K. Vandervoort, and J. Liu, Phys. Rev. Lett. **62**, 1908 (1989).
[11]J. M. Claassen, M. E. Reeves, and R. J. Soulen, Rev. Sci. Instrum. **63**, 996 (1991).
[12]D. B. Chrisey, J. S. Horwitz, H. S. Newman, M. E. Reeves, B. C. Weaver, K. S. Grabowski, and G. P. Summers, J. Superconduct. **4**, 57 (1991).
[13]M. K. Skrehot and K. Chang, IEEE Trans. Microwave Theory Tech. **MTT-38**, 434 (1990).
[14]R. L. Eisenhart, IEEE Trans. Microwave Theory Tech. **MTT-24**, 987 (1976).
[15]R. Karim, R. Seed, S. Oliver, A. Widom, and C. Vittoria, IEEE Trans. Magn. **MAG-25**, 3221 (1989).
[16]R. Karim, S. Oliver, C. Vittoria, G. Balestrino, S. Barbanera, and P. Paroli, J. Superconduct. **1**, 81 (1988).
[17]D. Saint-James, E. J. Thomas, and G. Sarma, *Type II Superconductivity* (Pergamon, New York, 1969).
[18]H. How, R. Seed, C. Vittoria, D. Chrisey, J. Horwitz, C. Carosella, and V. Folen, IEEE Trans. Microwave Theory Tech. **MTT-40**, 1668 (1992).
[19]D. Oates, A. Anderson, and Mankiewich, J. Superconduct. **3**, 251 (1991).
[20]M. R. Namordi, A. Mogro-Campero, L. G. Turner, and D. W. Hogue, IEEE Trans. Microwave Theory Tech. **MTT-39**, 1468 (1991).
[21]N. Klein, *High Temperature Superconductors,* edited by J. Pouch *et al.* (Trans. Tech., Aedermannsdorf, Switzerland, 1992).
[22]S. Sridhar and W. Kennedy, Rev. Sci. Instrum. **59**, 531 (1988).
[23]A. Portis, D. Cooke, and F. Gray, J. Superconduct. **3**, 297 (1991).
[24]J. Marteus, V. Hietaln, D. Ginley, T. Zipperian, and G. Hohenwarter, Appl. Phys. Lett. **58**, 2543 (1991).
[25]M. Tinkham, *Introduction to Superconductivity* (McGraw-Hill, New York, 1975).
[26]R. Karim, C. Vittoria, A. Widom, D. Chrisey, and J. Horwitz, J. Appl. Phys. **69**, 4891 (1991).
[27]P. de Trey and Suso Gygax, J. Low Temp. Phys. **11**, 421 (1973).
[28]D. Tilly, Proc. Phys. Soc. London **85**, 1177 (1965).
[29]J. Clem, Supercond. Sci. Technol. **5**, s33 (1992).
[30]T. Geballe and J. Hulm, Science **239**, 367 (1988).
[31]D. Harshman, L. Schneemeyer, J. Waszczak, G. Aeppli, R. Cava, B. Batlogg, and L. Rupp, Phys. Rev. B **39**, 851 (1989).
[32]D. Bishop, P. Gammel, D. Huse, and C. Murray, Science **255**, 165 (1992).
[33]L. Krusin-Elbaum, R. Greene, F. Holtzberg, A. Malozemoff, and Y. Yeshurun, Phys. Rev. Lett. **62**, 217 (1989).
[34]R. Cava, B. Batlogg, R. van Dover, D. Murphys, S. Sunshine, T. Siegrist, J. Remeika, E. Rietman, S. Zahurak, and G. Espinosa, Phys. Rev. Lett. **58**, 1676 (1987).
[35]A. Fiory, A. Hebard, P. Mankiewich, and R. Howard, Phys. Rev. Lett. **61**, 1419 (1988).

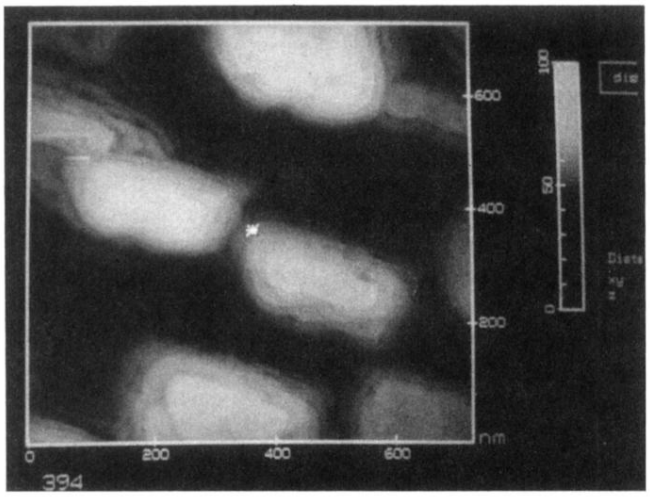

FIG. 1. STM micrograph of a superconducting film. The vertical and horizontal axes are in units of mm; each division is 200 nm.